THE DESIGN PROCESS AND SIMULATION TOOLS USED IN THE NEUTRONIC DESIGN OF THE ACR-1000® CORE

Adriaan Buijs
Atomic Energy of Canada Limited,
2251 Speakman Drive, Mississauga, ON L5K 1B2, Canada
buijsa@AECL.ca

ABSTRACT

This paper gives an overview of the design features and design process of the ACR-1000®[1], and in particular of the computing tools and techniques used in the design of the ACR-1000 core. The paper focuses on the neutronic design of the core, and describes how the codes WIMS-AECL[1], DRAGON[2], RFSP-IST[3] and MCNP[4] are used.

1. INTRODUCTION

The ACR-1000[5] is the Generation III+ design of AECL's line of CANDU®[2] reactors. The design retains many of the salient features of Classic CANDU reactors such as:

a. Fuel bundles located in horizontal pressure tubes;

b. Pressure tubes inside calandria tubes, located in a low-pressure D_2O moderator;

c. On-power refuelling.

Evolutionary design changes have been made with respect to Classic CANDU, such as thicker pressure tubes, an increase in the number of safety channels for the Regional Overpower Protection (ROP) from three to four, improved design of shut-off drives, etc. These design changes are based on operational experience with Classic CANDU, and better understanding of materials properties.

In additional, more significant changes to the design were made to respond to changing demands in safety and economic performance of the reactor. At the highest level, the changing demands are:

a. An increased emphasis on inherent safety to augment the engineered safety;

b. A shift from capital cost to operational cost.

[1] Advanced CANDU Reactor®, ACR® and ACR-1000® are trademarks of Atomic Energy of Canada Limited (AECL).

[2] CANDU® is a registered trademark of Atomic Energy of Canada Limited (AECL).

These high-level changes in design philosophy translate into the following changes in reactor design:

a. Enriched uranium is used for fuel;

b. Depleted heavy water (light water) is used for coolant;

c. The lattice pitch is reduced to a minimum of 24 cm required for single-tube replacement.

In terms of safety performance of the reactor, the consequences of the design changes are (when compared to Classic CANDU):

a. A distinctively negative power coefficient of reactivity (PCR);

b. A small reactivity effect due to voiding of the coolant system (CVR);

c. Reduced production of tritium in the heat-transport system;

d. Reduced volume of spent fuel.

Note that all engineered safety systems of the Classic CANDU are maintained as well. The economic consequences of the design changes are (when compared to Classic CANDU):

a. A significant reduction of the heavy water inventory (reduction of capital cost);

b. Increase of fuel manufacturing cost (operational cost);

c. Increase of fuel burnup;

d. Indirect cost savings through increased efficiency and reduction of waste.

2. NEUTRONIC SIMULATION OF CLASSIC CANDU

The neutronic simulation of a reactor core in Classic CANDU is based on the following three components:

a. Infinite-lattice calculations through a 2-D single-cell model with reflective boundaries using a neutron transport code such as WIMS-IST[6]. Burnup is performed in a lattice with critical buckling. These calculations yield information on intra-bundle power distributions and reactivity coefficients as a function of burnup, as well as a set of cross sections as functions of state parameters and as a function of burnup.

b. Incremental cross sections are calculated in a 3-D super-cell model. This is necessary because in CANDU reactors, the reactivity devices are perpendicular to the fuel elements. The incremental cross sections, typically calculated with the DRAGON code, are the difference in cross sections with and without the reactivity devices present[7].

c. The lattice-cell and incremental cross sections are stored in tables which are accessed by a 3-D code for full-core simulations, typically a finite-difference diffusion code using two energy groups, such as RFSP.

Most, if not all of the modelling requirements for CANDU reactors have been satisfied with the methodology described above.

Among the neutronic calculations that are possible with this code are:

a. Static calculations of flux, power (bundle and channel), k_{eff}, etc. under all possible operational conditions;

b. Time-average calculations. This calculation, applicable only to CANDU reactors, calculates the average thermal power in a fuel channel for a given average exit irradiation of the fuel in that channel. In an iterative process, it allows the analyst to calculate the exit burnup of the reactor for a given channel power distribution and fuelling scheme[8];

c. Core-follow calculations. Fuelling sequences can be simulated over long periods of time, in time-steps of typically a day. For a realistic simulation of the refuelling history, channels to be refuelled are chosen on the basis of criteria that are identical, or at least similar to those applied by the fuelling engineers at the plant;

d. Transient calculations are performed with the *CERBERUS module of RFSP in a quasi-static approximation, which entails that the overall flux shape in the core changes on a much longer timescale than the reactivity of the core. These calculations permit to study refuelling transients, xenon transients and accident transients such as LOCA;

e. Calculations of harmonic modes and flux detector response can be performed, as well as power and flux mapping, regulating system simulations and shutdown performance calculations. These assist in determining the ability for controlling and monitoring the reactor.

Calculations of the ACR-700 and initial calculations of the ACR were performed with the Classic – CANDU toolset described here. Soon after, changes to the computational toolset for the ACR-1000 were triggered by two circumstances:

a. The realisation that the current code set was not adequate to describe all pertinent features of the ACR-1000.

b. The emergence of the computer capacity to perform full-core Monte Carlo (MC) calculations.

These factors led to a change in methodology for design of the ACR-1000: A significant effort was spent in the improvement of the existing codes to accommodate ACR-1000 specific features and an increasing role was given to MC techniques, in particular MCNP, to assist in and verify the core design.

The remainder of this paper will discuss these developments.

At the same time, the need for proper validation of tools and methodologies specific to ACR-1000 arose. A major experimental program was set up to achieve this validation. This experimental program is outside the scope of this document.

3. THE ACR-1000 DESIGN PROCESS

3.1 Design Requirements

The design process of the ACR-1000 originates in a number of high-level requirements in terms of safety (based on Canadian and International standards and guidelines, such as RD-337 (Canada) and NS-R-1 (IAEA)) and economics (based on market requirements). These are cascaded down into system-specific design requirement documents. One such requirement is that "The maximum degree of positive reactivity and its maximum rate of increase by insertion in normal operation, AOOs, and DBAs are limited so that no resultant failure of the reactor pressure boundary will occur, cooling capability will be maintained, and no significant damage will occur to the reactor core." (RD 337)

This requirement translates into the safety requirement of a negative power coefficient of reactivity (PCR) and a coolant void reactivity sufficiently small that a power pulse due to a LOCA event does not lead to reactivity increase beyond prompt critical. Examples of economic requirements are an electrical output of at least 1165 MWe, and a burnup target of 20 MWd/kg(U). With safety limits on maximum channel powers, these translate into a requirement for the power form factor (average channel power over maximum channel power) of 0.94.

3.2 Design Implementation and its Effect on Neutronics

The safety design requirement mention above is achieved by the combination of reduced lattice pitch, enriched fuel, light water coolant, and a burnable neutron absorber in the center of the bundle. The neutronic effects of these changes are: (with respect to Classic CANDU)

a. A hardening of the neutron spectrum;

b. A steeper profile of thermal neutron flux radially across the fuel bundle, dropping essentially to zero at the boundary of the central absorber.

The hardening of the neutron spectrum in the moderator makes for a more negative fuel temperature coefficient in the ACR-1000 core than in a Classic CANDU: a relatively larger number of fast neutrons enter the bundle, where they are more readily absorbed in ^{238}U when the fuel temperature increases. The use of light water –needed to compensate for the loss of moderation in the moderator– by itself increases the coolant void reactivity significantly: in case of voiding, the absorption in light disappears and reactivity increases. The increase is compensated by absorption of thermal neutrons in the poison of the central pin. Under normal conditions, the central pin is shielded by the light water.

Note that this mechanism for CVR is different from that of Classic CANDUs: there, it is the absence of moderation due to the voided heavy water coolant that reduces the resonant absorption of neutrons in ^{238}U. Hence, adding a central poison pin does not have the same impact on CVR in Classic CANDU as in ACR-1000.

Another significant effect is that the voiding in one channel of the ACR-1000 affects the neutronic balance in the neighbouring channel to the extent that the reactivity increases when that neighbouring channel is not voided. This effect is called checkerboard CVR (or CBCVR) and occurs when one of the loops of the heat transport system voids due to an event such as an inlet-header break.

3.3 Design Requirements for Simulation Codes

The features mentioned in the previous section and others have led to formal design requirements for the codes. These are, among others:

a. The ability to perform multicell calculations: to be able to model the checkerboard effect, but also the reflector-core interface;

b. An improved resonance treatment: resonance absorption is more important in the ACR-1000;

c. Spatial treatment of resonance absorption;

d. Finer segmentation of the geometry: this requirement and the previous are mandated by the fact that the neutron spectrum is harder and varies more across a lattice cell;

e. The capability to simulate eccentric tubes: needed to model the effect of pressure tube sag;

f. The ability to model solid rod zone controllers;

3.4 Development of Improved Codes

3.4.1 WIMS

On the basis of the design requirements mentioned above –in addition to a number of technical requirements- the WIMS-IST (version 2.5d)[6] code has been rewritten as WIMS-AECL (version 3.1)[1]. An example of a multi-cell application is shown in Figure 1. It shows a geometry that involves the reflector as well as six fuel cells.

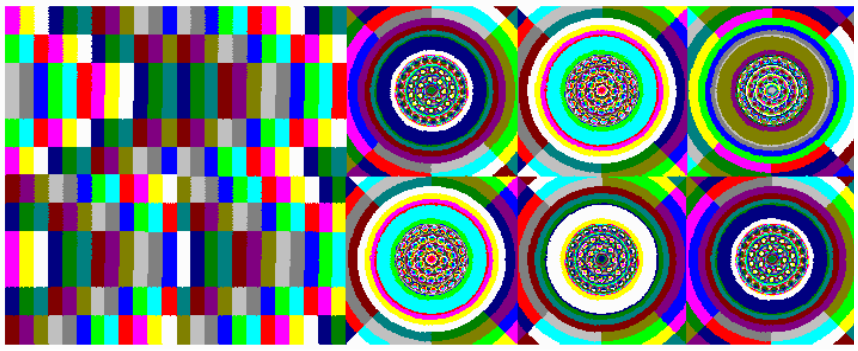

Figure 1: A multi-cell configuration in WIMS, including six fuel cells and the reflector.[13]

3.4.2 RFSP

The diffusion code RFSP[3] has been updated to accommodate the new features of the WIMS lattice code, as well as a number of other ACR-1000-specific features such as fuel temperature correlations. Other improvements, such as local parameters for moderator temperature, purity and poison concentration were also implemented. Finally, a new method for performing depletion calculations in the full-core simulations was developed, the micro-depletion method[9].

3.4.3 WIMS UTILITIES

The RFSP code is coupled to the WIMS lattice code through a set of utilities[10]. Among other things, the utilities condense the 89-group cross-sections into the two groups used by RFSP. They also perform a homogenization of cross sections over annular regions inside the cell used by RFSP (Fuel, coolant, moderator) or provide the data needed for the microdepletion method[9]. The interface between WIMS and RFSP is in the form of tables written by the WIMS utilities and read by RFSP.

3.5 External Design Codes

3.5.1 MCNP

MCNP[4] is a Monte-Carlo code which is increasingly important for code validation and design verification. It allows the user to build a model with an arbitrary level of detail – limited only by the number of cells that can be accommodated in the computer memory.

In the code, neutrons are generated and followed through the geometry under the influence of the physics processes governing scattering, absorption, fission etc. The cross sections applicable to the various physics processes are stored point-wise, as function of energy in the nuclear data library. The library currently used in the ACR-1000 design is the ENDF/B-VI library compiled by Brookhaven National Lab. The recently released version ENDF/B-VII of the libraries is being tested for use. The validation exercise for ACR-1000 is meant to confirm the applicability of these libraries to the ACR-1000 design.

The MNCP code is used for a variety of calculations at the level of a lattice cell as well as for the full core. Neutronic calculations are performed for k_{eff} determination, but also for establishing flux and power distributions.

At the lattice cell level, the MCNP code is used for:

a. Intrabundle power distribution: MCNP will track photons as well as neutrons, and gives therefore a more accurate description of the power inside the fuel bundle than a code such as WIMS. Whereas in WIMS all fission energy is deposited where the fission occurs, the MCNP code will track the portion of the energy carried away as neutrons and photons and deposit it where appropriate. In this manner, for example,

the power produced in the central poison pin –which is non-negligible– can be calculated;

b. End-flux peaking[11]: due to the absence of an absorber in the region between adjacent fuel bundles, the local flux in that region is significantly higher than say, in the region in the middle of the bundle. This effect is even stronger when there is only coolant adjacent to the bundle, as is the case during the refueling transient. MCNP is used to calculate the relative power along the bundle in each of the three rings of fuel elements. Note that the increased flux at the end of the bundle implies that burnup proceeds at a higher rate in this area. This means that 2-D cell calculations cannot be used to establish the isotope concentration in the pins, as these provide only an average over the bundle. For this reason, depletion calculations have been performed with the MONTEBURNS[12] package, which provides an extension to MCNP allowing for burnup calculations.

At the full-core level, the MCNP code is used for:

a. K-effective calculations for various core configurations, for example for
   i. Rod-worth determinations;
   ii. Coolant void reactivity (CVR);
   iii. Power coefficient of reactivity (CVR)
b. Flux-and-power calculations to verify the RFSP calculations.

The full-core model is obviously rather large, and the MCNP input file by itself cannot easily be edited or understood. To this end, a perl script was developed that allows the user to build the MCNP model of the ACR-1000 on the basis of design parameters. The script is rather versatile and allows to user to specify features such as creep and sag, and non-aligned fuel bundles.

The fuel composition of this model is obtained from WIMS lattice-cell burnup calculations. Given the complexity of the model, the burnup distribution over the core is binned in 64 or 100 bins, with one specific fuel composition for each bin. The MONTEBURNS procedure is still too time consuming to be practical for full-core models. The calculations are performed in parallel mode with MPI on a LINUX cluster with more than 100 nodes. However, it was found that the optimum parallel performance is achieved by running on about eight nodes simultaneously.

The k_{eff} calculation converges in a reasonable time (expressed in cycles and histories). However, the power (flux) distribution in such large models converges only slowly if at all, and shows an oscillatory behaviour even for a large number of cycles and histories. (This is visible in Figure 3) Methods exist to deal with these oscillations and obtain meaningful flux distributions and estimates of the statistical uncertainties in them. These methods involve either averaging over independent runs or averaging over core regions for which symmetries exist. The typical uncertainty for a channel power obtained in this way is of the order of 2%.

The MCNP applications described above concern the propagation of neutrons and photons. In addition, MCNP can be used for transport of electrons. In the ACR-1000 design, this feature is used to model the response of detectors in the reactor and in the test-reactor ZED-2.

4. THE ACR-1000 CORE DESIGN

4.1 The Time-Average Core

The calculation of the time-average core is at the basis of the core design, as it is in Classic CANDU[8]. For the ACR-1000, the time-average calculation yields the power distribution shown in Figure 2[5]. Note that this distribution implies a certain location for the reactivity devices, which are assumed to be at mid-insertion for this calculation. While the time-average calculation itself is an iterative process, establishing the locations of the reactivity devices is an iterative procedure as well, based on a number of considerations: the axial flux shaping in the channels, controllability of the reactor, physical placement of the drives, and physical placement with respect to other devices such as shut-off rods and GSS rods. This makes the overall iterative process for the time-average core somewhat cumbersome. Furthermore, at present no formal algorithm was applied to optimize the location of the controllers. The current location is based on experience and trial-and-error, and optimized by iteration.

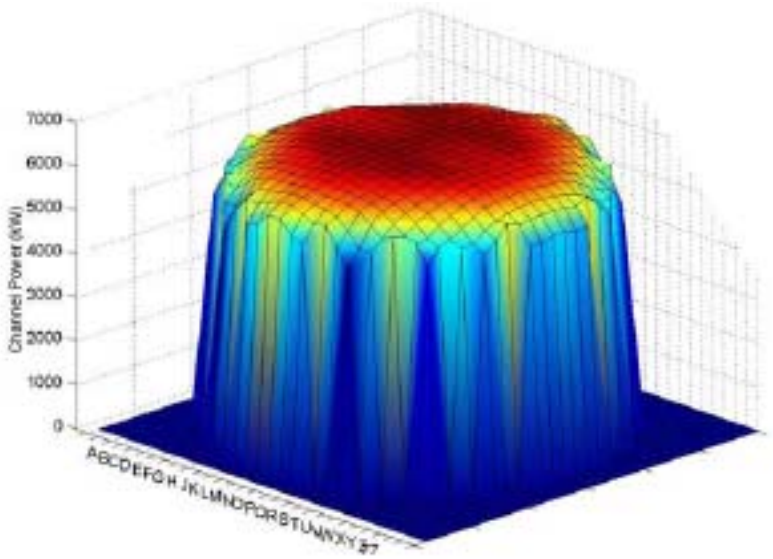

Figure 2: Time-Average channel power distribution.[5]

The time-average core does not represent a physical state of the core at any time. In order to obtain such a snapshot, each channel must be assigned a random age, and each bundle a definite value of burnup. There are infinitely many different instantaneous cores possible, and in principle, a large number of such cores (called INSTANTAN cores) would be representative for the ACR-1000 core over a long period.

A comparison with MCNP was made as a verification of the power calculations with the standard toolset WIMS/DRAGON/RFSP. To this end, the MCNP model was generated with the same isotopic compositions as the RFSP model (i.e. both models were generated with isotopic compositions according to burnup values that were binned in 64 or 100 bins). Figure 3 shows the results of the comparison for a row of channels across the face of the core. It is seen that the agreement is better than 2%, and that most disagreement appears near the edge of the core, at the core-reflector interface. Note that the same comparison with the old single-cell methodology of WIMS shows a much worse agreement, confirming that the single-cell methodology is inadequate for design of the ACR-1000. Note also that the remaining discrepancy does not reflect the operational channel power uncertainty. The latter is determined by the ability to map the flux and measure the power. The design uncertainty is ultimately reflected in a burnup uncertainty.

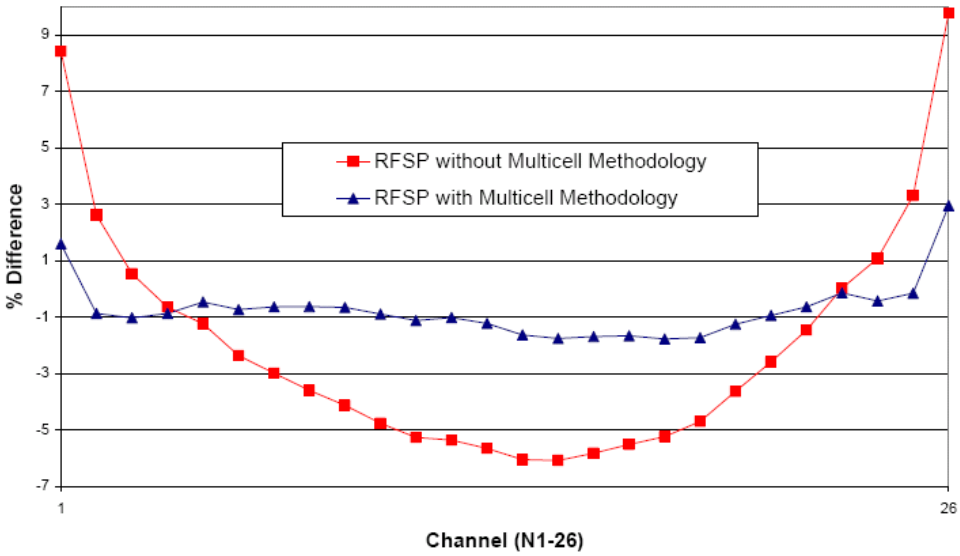

Figure 3: Comparison of channel power calculations between RFSP and MCNP for channels on the center-line of the core[13].

4.2 Reactivity Coefficients

Reactivity coefficients are defined as the changes in reactivity as a result of a change in state parameter divided by the change in that state parameter. Examples are moderator temperature, moderator purity, moderator poison, coolant temperature, coolant density (not coolant purity anymore!), fuel temperature. In practice, the coefficients are calculated by performing a calculation at nominal conditions, and one at sufficiently perturbed conditions.

Reactivity coefficients are calculated with WIMS to show the dependence of the coefficient on burnup. These are obviously unphysical coefficients, since they are valid only

for an infinite lattice of bundles with identical burnup, but they provide information on the behaviour of the coefficient.

Realistic reactivity coefficients are calculated with RFSP (and verified with MCNP). These calculations show the reactivity properties of the core with a realistic mix of burnups.

Full-core RFSP and MCNP calculations are also used to track the change of reactivity coefficients as a function of core age. As the core ages, the pressure tube diameter increases; this causes the coolant volume to increase and changes the cooling properties of the bundles, since water will bypass the bundle more easily. In fact, the end of life of the pressure tube is defined as the point in time where the safety margins have been eroded to the point where power de-rating becomes necessary. Currently, the life time is 30 years, after which the pressure tubes must be replaced. As a result, all safety related calculations are performed with fully crept pressure tubes at end of life.

4.3 Coolant Void Reactivity

Of particular interest is the reactivity insertion due to voiding of the fuel channels. As described earlier, the effect of this voiding is the net result of a large positive contribution (loss of absorption in light water) and a large negative contribution (increased absorption in the central pin). In addition, there are several contributions from the uranium and plutonium isotopes as well. Although the reactivity contributions almost cancel, the uncertainties on the contributions accumulate. As a consequence, the uncertainty on the CVR can be significant, even if its value is zero.

An extensive program has been set up to establish with high confidence that the CVR of the ACR-1000 will be small and negative under nominal operating conditions. The components of this program are:

a. Extensive validation of the codes in CVR experiments with the ZED-2 facility at AECL Chalk River Laboratories. Fuel similar to ACR-1000 fuel, both fresh and at mid-burnup (MOX) is used in geometries identical to those of ACR-1000, under cooled and voided conditions. In the experiments, both configurations are made critical by adjustment of the moderator height. Corresponding calculations are performed with MCNP, including the voiding conditions and measured critical heights. Ideally, both calculations should yield $k_{eff} = 1$. In practice, there is a difference; both numbers are a few mk below 1 and different from each other. The latter difference is defined as the bias in the code.

b. Uncertainties in the bias are established. Although the bias itself is thought to be almost fully caused by errors in the nuclear cross sections, the error in the bias is due to experimental uncertainties. These are estimated, or more rigorously calculated using the GRS method[14], which will be described later.

c. A methodology exists to establish the similarity between a test reactor and an actual power reactor. This methodology, implemented in the TSUNAMI code[15], calculates the sensitivity of a system to errors in the nuclear data. If the sensitivities of

the k_{eff} of two different systems (ZED-2 and ACR-1000) are similar, the two systems are said to be neutronically similar. The TSUNAMI code has been modified to allow for similarity calculations of reactivity perturbations, thus allowing us to establish the similarity of ZED-2 and ACR-1000 for CVR. Preliminary results confirm that they are similar. The TSUNAMI method also provides a tool to extend the bias and uncertainty of ZED-2 measurements to ACR-1000 conditions.

The bias and uncertainty on the CVR calculation with MCNP in ZED-2 are translated to a bias and uncertainty for ACR-1000 conditions as described in the previous items. These are applied in different manners in two analyses:

a. To establish the 95%/95% limit on the actual value of CVR under nominal conditions. Here, again the GRS method is applied, which takes into account all operational uncertainties of the ACR-1000 reactor. This calculation is performed with MCNP.

b. The central value for CVR as calculated by MCNP for ACR-1000 is corrected for the bias and augmented conservatively by two standard deviations. This limiting value is used to adjust the CVR calculated by RFSP for the same conditions. RFSP, with those conditions is then used to perform the safety analysis calculations.

4.4 The Power Coefficient

The other key reactivity effect is the power coefficient of reactivity (PCR). It is mainly determined by the Doppler broadening of resonances in the ^{238}U neutron absorption. As mentioned before, the ACR-1000 neutron spectrum is harder than that of Classic CANDU; hence, more fast neutrons penetrate the fuel from the moderator which increases the chance of absorption in broadened resonances.

In order to perform an assessment of the uncertainty in the PCR under operating conditions, the GSS method was applied, as for the CVR. Since the PCR is very sensitive to the thermalhydraulic conditions, calculations of the coolant conditions (and their effect on the fuel temperature) were calculated by ELESTRES[16] for each run in the study. Calculations were done both with RFSP and with MCNP, both showing that the power coefficient is negative with greater than 95% probability under 95% confidence level.

Validation experiments for PCR with heated channels in ZED-2 are scheduled to take place with cores of ACR-1000-like fuels. Verification of the power coefficient with the FUGEN experiment[19] is taking place, and preliminary results show agreement.

4.5 Core Performance and Margins

The core performance characteristics were not derived from the time-average core or the INSTANTAN core but rather from individual snapshots taken during a core-follow study[20]. A script was developed that selects channel to be refuelled on the basis of a number of criteria that are similar to the ones the fuelling engineer at the station would use. The results of this

core follow in terms of channel powers and bundle powers are shown in Figure 4. The maximum channel powers are limited and well below the design basis limit.

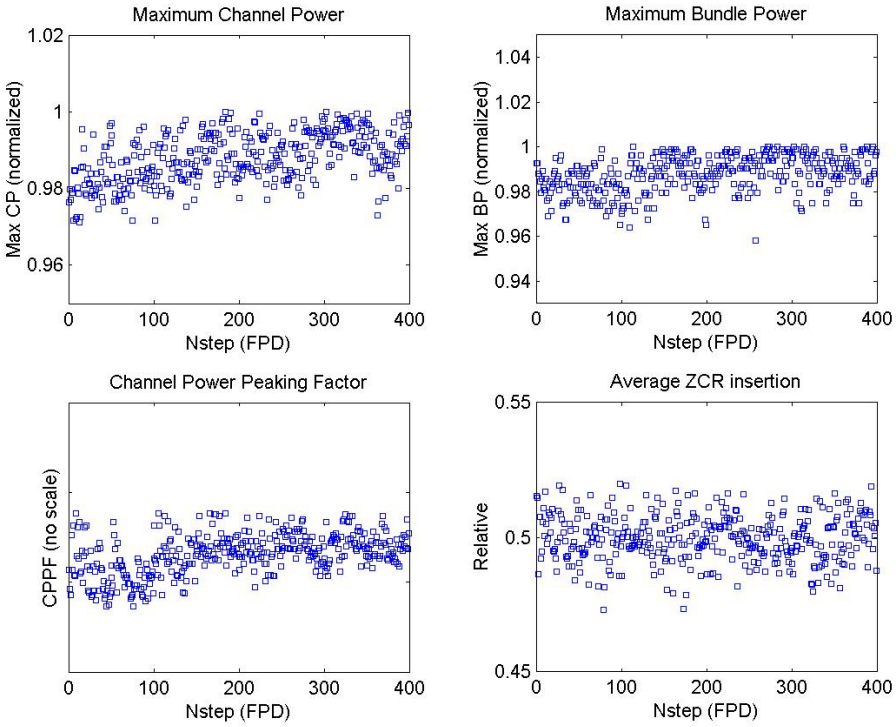

Figure 4: Results from a core-follow study: channel and bundle powers, channel power peaking factor and average zone controller insertion.[20]

The data obtained from the core-follow are used to study operational aspects of the core design such as refuelling transients. Figure 5 shows the transient in terms of bundle powers for a complete refuelling cycle. It is seen that the bundle power increases as the fuel string traverses the core and reaches a maximum at position 8. These calculations are performed with RFSP, including the effect of fuel temperature feedback and reactor regulating system (RRS). The bundle powers thus obtained are fed back to the fuel design group to determine the margin to melting. Worst case scenarios show that the refuelling transients are acceptable for the current fuel design.

Step	Channel Power (kW)	Bundle Power in Channel H12 (kW)											
		1	2	3	4	5	6	7	8	9	10	11	12
0	6122	243.3	568.0	682.8	688.9	652.8	591.7	562.9	565.1	537.1	488.8	382.4	158.5
1	6420	232.6	593.5	716.1	724.8	697.1	629.0	601.3	601.1	565.4	507.8	393.6	158.5
2	6704	228.6	561.3	739.6	766.9	745.5	674.4	639.9	641.1	596.5	534.2	412.3	164.0
3	6742		551.4	700.1	799.2	796.8	723.3	686.0	680.5	631.9	563.8	436.8	172.4
4	6437			687.3	762.5	832.7	774.0	735.9	728.9	668.9	599.0	464.6	183.6
5	5976				779.0	793.4	807.9	785.9	778.4	711.6	631.5	493.3	195.1
6	5346					767.5	760.4	817.0	830.5	760.9	676.1	525.4	209.1
7	4689						732.6	767.9	862.7	812.1	725.3	565.2	223.7
8	4022							738.9	810.1	844.8	777.3	609.2	241.8
9	3310								781.6	798.9	813.9	654.8	261.1
10	2517									780.9	774.8	682.9	278.8
11	1693										767.1	641.7	284.7
12	2517									780.9	774.8	682.9	278.8
13	3310								781.6	798.9	813.9	654.8	261.1
14	4022							738.9	810.1	844.8	777.3	609.2	241.8
15	4689						732.6	767.9	862.7	812.1	725.3	565.2	223.7
16	5346					767.5	760.4	817.0	830.5	760.9	676.1	525.4	209.1
17	5976				779.0	793.4	807.9	785.9	778.4	711.6	631.5	493.3	195.1
18	6437			687.3	762.5	832.7	774.0	735.9	728.9	668.9	599.0	464.6	183.6
19	6742		551.4	700.1	799.2	796.8	723.3	686.0	680.5	631.9	563.8	436.8	172.4
20	6704	228.6	561.3	739.6	766.9	745.5	674.4	639.9	641.1	596.5	534.2	412.3	164.0

Figure 5: Channel and bundle powers during the refuelling transient.
The highest bundle powers are highlighted in yellow.[21]

5. COMPUTATIONAL TECHNIQUES AND OPTIMIZATIONS

5.1 The GRS method

The GRS method is based on Wilks' formula[14]: This formula yields the number of random samples n that are needed to obtain limits on a given value computed as a function of an arbitrary number of input parameters. For one-sided tolerance limits: $1-\alpha^n \geq \beta$, where $\beta\times100$ is the confidence level (%) that the maximum code result will not be exceeded with the probability $\alpha\times100$ (%) (fractile) of the corresponding output distribution, which is to be compared to the acceptance criterion. The confidence level is specified to account for the possible influence of the sampling error due to the fact that the statements are obtained from a random sample of limited size. For two-sided statistical tolerance intervals the formula is: $1-\alpha^n-n\,(1-\alpha)\,\alpha^{n-1} \geq \beta$. The limits are quoted as probabilities at a given confidence level. For example, in order to obtain a one-sided 95/95 limit, a total of n=59 random samples need to

be generated. The highest (lowest) value of this sample would be the upper (lower) limit. Note that only one of the two limits is obtained in this way. If a double-sided limit is needed, a total of 93 samples need to be generated. Some, limited, information about trends and dependencies of the results to the input parameters can be obtained in this method as well. The limits obtained cannot easily be converted to uncertainties, since the distribution of samples is not necessarily Gaussian. As mentioned above, the GRS method is applied in the study of CVR and PCR.

5.2 Simulated Annealing

A number of design features in a reactor core lend themselves to the use of modern design algorithms. One such algorithm is simulated annealing[17]. In this method, an objective function is defined such that its value is lower according to the degree with which the design matches the requirements; a value of zero implies a perfect match. An iterative cycle is generated, in which quasi-random changes to the design are evaluated through the objective function. A number of criteria is used to decide if the changes are kept. The cycle continues until a predefined level of convergence is obtained, i.e. until no further improvement is observed.

The simulated annealing has been applied in two areas of the core design: the layout of the ROP detectors and the definition of the initial core.

6. NUCLEAR DESIGN VERIFICATION

An extensive program is in place to verify the core physics design of the ACR-1000. The verification is performed according to the Canadian standard CSA 286.2, which specifies a number of verification techniques. Some of these, such as independent verification, review and comment, and design walk-through have been applied as the design progressed.

For the verification of the design and the tools through independent calculation an alternate toolset was acquired by the Office of the Chief Engineer of AECL. This code set consists of the British codes WIMS9 (no longer related to the AECL version of WIMS), PANTHER[18] and MONK (developed by SERCO Assurance and British Nuclear Fuel). WIMS9 is a lattice cell code, PANTHER a multi-group diffusion code, and MONK a Monte Carlo code with continuous energy as well as multi-group capabilities. The codes use the European JEF-2.2 nuclear data libraries. Preliminary calculations of ACR-1000 core properties confirm the validity of our codes and design calculations.

In addition, experimental verification is being performed on data obtained from the FUGEN reactor[19]. The FUGEN reactor was a prototype MOX burning reactor in Japan. It is similar to ACR in that it has:

a. 24 cm lattice pitch with similar pressure tube and calandria tube dimensions;

b. Enriched fuel in a geometry similar to the ACR fuel geometry;

c. Light water coolant;

d. Heavy water moderator.

A large number of experiments have been performed with the FUGEN reactor, including measurements of flux distributions, of CVR and PCR. AECL has acquired data sets for a number of cycles and is analysing the experiments with RFSP and MCNP.

7. CONCLUSION

The ACR-1000 core design is a top-down design, based on a formal set of requirements, processes and operating instructions. A number of new or improved design tools have been introduced for the ACR-1000 design, some of which were provided in-house (i.e. by AECL) like WIMS-AECL and RFSP, and some of which are external, like MCNP. The design tools and a number of new design techniques such as GRS, TSUNAMI and simulated annealing are adequate to address all design features that distinguish the ACR-1000 from the Classic CANDU reactors. A major validation exercise is currently being undertaken, based on the experimental reactor ZED-2 at the Chalk River Laboratories. The Japanese prototype reactor FUGEN is being considered as one of the methods for verification of the design.

REFERENCES

1. Altiparmakov, D., “New Capabilities of the Lattice Code WIMS-AECL”, International Conference on Reactor Physics, Interlaken, Switzerland, September 14-19, 2008; and Shen W., “Development of a Multicell Methodology to Account for Heterogeneous Core Effects in the Core-Analysis Diffusion Code”, American Nuclear Society's Topical Meeting on Reactor Physics: Advances in Nuclear Analysis and Simulation, PHYSOR-2006, Vancouver, British Columbia, September 10-14, 2006.
2. Marleau, G., Hébert A. and Roy R., “A User Guide for DRAGON Version DRAGON_000331 Release 3.04”, Report IGE-174 Rev. 5, Institut de Génie Nucléaire, École Polytechnique de Montréal, Montréal, Québec, 2000.
3. Rouben, B., “RFSP-IST, The Industry Standard Tool Computer Program for CANDU Reactor Core Design and Analysis”, in the Proceedings of the 13th Pacific Basin Nuclear Conference, Shenzhen, China, 2002.
4. X5-MCNP-Team, “MCNP – A general Monte Carlo N-particle transport code, version 5”, Volume I: Overview and theory. Tech. Rep. LA-UR-03-1987, Los Alamos National Laboratory, 2000.
5. Buijs, A., et al., “The Physics Design of the Advanced CANDU Reactor”, International Conference on the Physics of Reactor, Interlaken, Switzerland, September 14-19, 2008.
6. Irish, J.D. and Douglas S.R., “Validation of WIMS-IST”, in the Proceedings of the 23rd Annual Conference of the Canadian Nuclear Society, Toronto, Ontario, Canada, 2002.

7. Dahmani, M., et al., “WIMS-IST/DRAGON-IST Side-Step Calculation of Reactivity Device and Structural Material Incremental Cross Sections for Wolsong NPP Unit 1”, these proceedings.
8. Rouben B., “Review Of The CANDU Time-Average Model And Calculations”, in the Proceedings of the 28th Annual CNS Conference, St. John, New Brunswick, 2007.
9. Shen, W., “Development of a Micro-Depletion Model to Use WIMS Properties in History-Based Local-Parameter Calculations in RFSP”, in the Proceedings of the Sixth International Conference on Simulation Methods in Nuclear Engineering, Montréal, Québec, Canada, 2004.
10. Liang, T., Shen, W., Varin, E., Ho., K., “Improvements and Qualification of WIMS Utilities”, Proceedings of the 29th Annual CNS Conference, Toronto, Ontario, June 2008.
11. Hill, I., Donnelly, J.V., “MCNP Simulations of End Flux Peaking in ACR-1000, 2.4 wt % ^{235}U Fuel Bundles”, in the Proceedings of the IYNC 2008, Interlaken, Switzerland, 20-26 September 2008.
12. Radiation Safety Information Computational Centre, ORNL, Oak Ridge, Tennessee, “MONTEBURNS 2.0: An Automated, Multi-Step Monte Carlo Burnup System”, PSR-455, July 2003; and
Radiation Safety Information Computational Centre, ORNL, Oak Ridge, Tennessee, “ORIGEN 2.2: Isotope Generation and Depletion Code Matrix Exponential Method”, CCC-371, June 2002.
13. Shen, W., et al., “Benchmarking of WIMS-AECL/RFSP Multicell Methodology with MCNP for ACR-1000 Full-Core Calculations”, International Conference on the Physics of Reactors, Interlaken, Switzerland, September 14-19, 2008.
14. Glaeser, H., “Uncertainty Evaluation of Thermal-Hydraulic Code Results”, International Meeting on “Best-Estimate” Methods in Nuclear Installation Safety Analysis (BE 2000), Washington, DC, 2000; and
Hofer, E., “Probabilistische Unsicherheitsanalyse von Ergebnissen umfangreicher Rechenmodelle GRS-A-2002", 2002; and
Wilks, S., “Statistical Prediction with Special Reference to the Problem of Tolerance Limits”, paper presented at a joint session of the American Mathematical Society and the Institute of Mathematical Statistics at Poughkeepsie, 1942.
15. Broadhead, B.L., Rearden, B.T., Hopper, C.M., Wagschal, J.J. and Parks, C.V., “Sensitivity- and Uncertainty-Based Criticality Safety Validation Techniques”, *Nucl. Sci. Eng*. **146**, 340–366 (2004); and
Rearden, B.T., “Perturbation Eigenvalue Sensitivity Analysis with Monte Carlo Techniques”, *Nucl. Sci. Eng*. **146**, 367–382 (2004); see also
http://www.ornl.gov/sci/scale/tsunami/references.shtml
16. Wong, H.H., Alp E., Clendening, W.R., Tayal, M., Jones, L.R., “ELESTRES: a finite element fuel model for normal operating conditions”, *Nuclear Technology*, Vol. 57, Iss. 2, pp. 203-212 (1982).
17. Kirkpatrik, S., Gelatt, C., and Vecchi, M., “Optimization by Simulated Annealing,” *Science*, **220**, 671-680, (1983).

Press, W.H. *et. al.* "Numerical Recipes in FORTRAN 77: the Art of Scientific Computing," 2nd Ed., Volume 1, p. 436, (1992).

18. Hutt, P.K., Gaines, N., Halsall, M.J., McEllin, M., White, R.J., "The UK Core Performance Code Package". Nuclear Energy, British Nuclear Energy Society, 30, 291, 1991;
    Newton, T.D., Hutton, L. J., "The Next Generation WIMS Lattice Code: WIMS9", in the Proceedings of the PHYSOR 2002, Seoul, Korea, 2002.
19. Ohtani, T., Iijima, T., Shiratori, Y., "Analysis of Mixed Oxide Fuel Loaded Cores in the Heavy Water Reactor FUGEN", *J. of Nucl. Sci. and Technol.*, Vol. 40, no. 11, p.959-969 (2003).
20. Farkas, R., Robinson, R, Rehman, A. and Buijs, A., "Simulation of Long-Term Fuelling Operations for the ACR-1000", Proceedings of the 29th Annual CNS Conference, Toronto, Ontario, June 2008.
21. Hu, J., Martchouk, I. and Robinson, R., "RFSP-IST Simulation of Fuel Transient During Refuelling the ACR-1000 Reactor", Proceedings of the 29th Annual CNS Conference, Toronto, Ontario, June 2008.